Empty Level Structure and Dissociative Electron Attachment Cross Sections in Saturated and Unsaturated Bromohydrocarbons

Alberto Modelli*,† and Derek Jones‡

Dipartimento di Chimica "G. Ciamician", Università di Bologna, via Selmi 2, 40126 Bologna, Italy, Corso di Laurea in Scienze Ambientali, Piazza Kennedy 12, 48100 Ravenna, Italy, Istituto per la Sintesi Organica e la Fotoreattività (ISOF), C. N. R., via Gobetti 101, 40129 Bologna, Italy

Received: September 15, 2003; In Final Form: November 17, 2003

The gas-phase electron transmission (ET) and dissociative electron attachment (DEA) spectra are reported for nine (normal, secondary, and tertiary) bromoalkanes and ten bromoalkenes where the bromine atom is directly bonded to an ethene carbon atom or separated from the double bond by 1−4 CH_2 groups. The relative DEA cross sections (essentially due to the Br^- fragment) are reported and compared with those of the corresponding chlorides. B3LYP/6-31G* calculations are employed to evaluate the virtual orbital energies (VOEs) for the optimized geometries of the neutral states of the bromohydrocarbons. The calculated VOEs satisfactorily reproduce the trends of the vertical electron attachment energies (VAEs) measured in the ET spectra. Electron attachment to the σ^*_{C-Br} MO of the saturated bromides occurs at about 1.2 eV, the energy of the resonance being slightly stabilized with increasing branching. The corresponding peak in the DEA cross section occurs at about 0.6 eV in the normal bromoalkanes and 0.9 eV in the secondary and tertiary bromoalkanes. In vinyl bromide, the lowest resonance is associated with the ethene π^* LUMO, whereas in the $CH_2{=}CH(CH_2)_nBr$ alkenes with $n > 2$, the LUMO is the σ^*_{C-Br} MO. Consistently, in the latter compounds the energy at the peak of the DEA cross section and the magnitude of the latter are comparable to those of the normal bromoalkanes.

Introduction

Electron−molecule (atom) collisions play an important role in various scientific fields, from both theoretical and technological points of view.[1] An important improvement in the detection and characterization of unstable gas-phase anions came about with the electron transmission spectroscopy (ETS) apparatus devised by Sanche and Schulz,[2] which favored the study of temporary anion formation in (relatively large) molecular systems of chemical interest[3] and is still one of the most suitable means for measuring negative electron affinities (EAs).

The ETS technique takes advantage of the sharp variations in the total electron−molecule scattering cross section caused by resonance processes, namely, temporary capture of electrons with appropriate energy and angular momentum into empty molecular orbitals (MOs).[3,4] Electron attachment is rapid with respect to nuclear motion, so that temporary anions are formed in the equilibrium geometry of the neutral molecule. The measured vertical attachment energies (VAEs) are the negative of the vertical EAs. These data are thus complementary to the ionization energies supplied by photoelectron spectroscopy. A complete picture of the frontier orbital structure (on which the most important molecular properties depend) can only be provided by the use of both techniques.

Additional information on temporary negative ion states can be supplied by dissociative electron attachment spectroscopy (DEAS),[4,5] which measures the yield of negative fragments as a function of the incident electron energy. When suitable energetic conditions occur, the decay of unstable molecular anions formed by resonance can follow a dissociative channel which generates long-lived negative fragments and neutral radicals, in kinetic competition with simple re-emission of the extra electron: $e^-_{(E)} + AX \rightarrow AX^{-*} \rightarrow A + X^-$.

An application of particular interest of DEAS, in conjunction with ETS, consists of its use as a probe for intramolecular electron-transfer processes, when an incident electron is first trapped into a localized functional group and then transferred to a remote group (or atom) where bond dissociation and formation of a negative fragment takes place. Such long-range electron transfer processes play an important role in photochemistry and biochemistry. In addition, systems capable of transmitting variations of charge density between different parts of a molecule are increasingly important in the field of nanoscale technology, i.e., organic conductors, molecular wires, and molecular devices.[6]

Most of the studies of electron attachment to halo compounds have been devoted to chloro derivatives. In the DEA spectra of unsaturated chlorohydrocarbons, the maximum yield of chloride negative fragments occurs close to the energy of the lowest π^* resonance observed in ETS,[7−19] suggesting that the Cl^- yield reflects the efficiency of intramolecular electron transfer from the π system (where the extra electron is first trapped) to the remote chlorine atom.

Moore and co-workers[16] showed that in the chloroalkenes $CH_2{=}CH(CH_2)_nCl$ the Cl^- current associated with the π^* resonance rapidly decreases with increasing length of the alkyl chain, due to the high energy of the empty σ^*_{C-C} orbitals and their consequent inability to promote coupling between the π^* and σ^*_{C-Cl} orbitals. In the same DEA study,[16] the cross sections of the corresponding bromoalkenes were also measured (to our

* To whom correspondence should be addressed. Phone: +39 051 2099522. Fax: +39 051 2099456. E-mail: modeli@ciam.unibo.it.
† Università di Bologna and Corso di Laurea in Scienze Ambientali.
‡ Istituto per la Sintesi Organica e la Fotoreattività.

10.1021/jp036744r CCC: $27.50
Published on Web 12/20/2003

knowledge, the only data reported in the literature on this class of compounds). The authors observed that the energy at the peak of the Br^- cross section decreases with chain length, whereas its magnitude decreases less rapidly than in the chloro analogues. These findings were ascribed to a stabilization of the π^* LUMO in the bromoalkenes as the alkyl chain becomes longer, together with a larger σ^* component with respect to the chlorides.

We have recently studied the empty level structure and DEA in analogous series of chloroalkyl derivatives of benzene,[17,18] ethene, and ethyne[19] and compared the Cl^- currents with those measured in saturated chloroalkanes, where production of the chloride anion derives directly from dissociation of the lowest σ^* resonance (VAE = 2.39 eV in 1-chlorobutane[20]). Although the magnitude of the DEA cross section is affected by the π functional, on going from the $-CH_2Cl$ (where the greatest σ^*_{C-Cl}/π^* mixing occurs) to the $-(CH_2)_3Cl$ derivative of each π system, the Cl^- current decreases by more than 2 orders of magnitude,[18,19] becoming intermediate between those measured in (saturated) normal and secondary chloroalkanes.

Here we extend the study of the empty level structure and the measurements of the DEA cross sections to unsaturated and normal, branched, and cyclic saturated bromohydrocarbons. To our knowledge, the only DEA study on saturated bromides, except for bromomethanes, is a swarm-beam study of normal bromoalkanes by Christophorou et al.[21]

ETS showed that the lowest σ^*_{C-Br} resonance of saturated bromohydrocarbons lies at sizably lower energy than the corresponding σ^*_{C-Cl} resonance of the chloro analogues.[22] The consequently longer lifetime of the σ^*_{C-Br} resonance is expected to favor its dissociative decay channel. In agreement, the absolute DEA cross sections reported for normal bromoalkanes[21] are about 30 times larger than those measured in the corresponding chlorides.[23] The ET spectra of bromoalkanes and bromoalkenes, interpreted with the support of theoretical calculations, and comparison of the VAEs with the energies of the peaks in the DEA spectra, as well as the relative DEA cross sections, are expected to provide more insight into the empty level structure and the dissociative mechanism (i.e., the role played by the π^* and σ^* resonances) in the unsaturated bromides.

A theoretical approach adequate for describing the energetics of unstable anion states involves difficulties not encountered for neutral or cation states. A proper description of spatially diffuse species requires a basis set with diffuse functions. However, as the basis set is expanded, an SCF calculation ultimately describes a neutral molecule and an unbound electron in the continuum.[24] Stabilization procedures are then needed to distinguish the virtual orbitals which give rise to temporary anion states from those low-energy solutions having no physical significance with regard to the resonance process.[24−27]

The Koopmans' theorem (KT) approximation[28] neglects correlation and relaxation effects. However, Staley and Strnad[24] demonstrated the occurrence of good linear correlations between the $\pi^*_{C=C}$ VAEs measured in a large number of alkenes and benzenoid hydrocarbons and the corresponding virtual orbital energies (VOEs) of the neutral molecules obtained with simple KT-HF calculations, using basis sets which do not include diffuse functions. The same linear equations nicely reproduce the $\pi^*_{C=O}$ VAEs measured in mono- and diketones.[29]

We have recently shown[19] that also the neutral state π^* VOEs obtained with B3LYP/6-31G* calculations supply a good linear correlation with the VAEs measured over a variety of different families of unsaturated compounds. Here we verify whether the B3LYP π^* VOEs scaled with the same equation can supply a good quantitative prediction of the VAEs measured in the bromoalkenes studied here and whether the σ^* VOEs parallel the energy trends of the corresponding features displayed in the ET spectra.

Experimental Section

Our electron transmission apparatus is in the format devised by Sanche and Schulz[2] and has been previously described.[30] To enhance the visibility of the sharp resonance structures, the impact energy of the electron beam is modulated with a small ac voltage, and the derivative of the electron current transmitted through the gas sample is measured directly by a synchronous lock-in amplifier. The present spectra were obtained by using the apparatus in the "high-rejection" mode[31] and are, therefore, related to the nearly total scattering cross section. The electron beam resolution was about 50 meV (fwhm). The energy scale was calibrated with reference to the $(1s^12s^2)$ ^2S anion state of He. The estimated accuracy is ± 0.05 or ± 0.1 eV, depending on the number of decimal digits reported.

The collision chamber of the ETS apparatus has been modified[9] in order to allow for ion extraction at 90° with respect to the electron beam direction. Ions are then accelerated and focused toward the entrance of a quadrupole mass filter. Alternatively, the total anion current can be collected and measured (with a picoammeter) at the walls of the collision chamber (about 0.8 cm from the electron beam). Although the negative ion current at the walls of the collision chamber can, in principle, be affected by spurious trapped electrons, these measurements are more reliable with respect to the current detected through the mass filter because of kinetic energy discrimination in the anion extraction efficiency in the latter experiment. In a previous test[32] with several monochloro alkanes, our relative total anion currents reproduced to within 1% the ratios in the absolute cross sections reported by Pearl and Burrow.[23]

The DEAS data reported here were obtained with an electron beam current about twice as large as that used for the ET experiment. The energy spread of the electron beam increased to about 120 meV, as evaluated from the width of the SF_6^- signal at zero energy used for calibration of the energy scales.

The relative total anion currents were evaluated from the peak heights, normalized to the same electron beam current and sample pressure (measured in the main vacuum chamber by means of a cold cathode ionization gauge) for all compounds. Preliminary measurements showed that the total anion current reading is linearly proportional to the pressure, at least in the $10^{-5}-4 \times 10^{-5}$ mbar range.

The calculations were carried out with the Gaussian 98 set of programs.[33] The geometry optimizations and electronic structure calculations on the neutral molecules were performed using the B3LYP density functional method[34] with the standard 6-31G* basis set. The calculated VAEs were obtained as the difference between the total energy of the neutral and that of the lowest anion state, both in the optimized geometry of the neutral state.

All of the compounds were commercially available. 4-Br-2-butene was an admixture of cis and trans isomers.

Results and Discussion

Calculated Molecular Geometries. The geometries of the neutral molecules were optimized with B3LYP calculations, using the 6-31G* basis set. The geometrical parameters which more directly affect the energies of the empty σ^*_{C-Br} and $\pi^*_{C=C}$ MOs are respectively the C−Br bond length and the distance

TABLE 1: Calculated Bond Distances (Å), Neutral State Virtual Orbital Energies (VOEs), Scaled (See Text) π^* VOEs (in Parentheses), and Calculated VAEs (Energy Difference between the Lowest Anion and the Neutral State, Both in the Optimized Geometry of the Neutral Molecule)[a]

	B3LYP/6-31G*					ETS
	d_{C-Br}	$d_{C=C}$	orbital	VOE	VAE	VAE (fwhm)
CH_3CH_2Br	1.9850		σ^*_{C-Br}	0.119	2.58	1.26[b] (1.1)
$CH_3CH_2CH_2Br$	1.9893		σ^*_{C-Br}	0.154	2.56	1.3 (1.2)
$CH_3CH_2CH_2CH_2Br$	1.9900		σ^*_{C-Br}	0.151	2.51	1.3 (1.2)
$CH_3CH(Br)CH_3$	2.0087		σ^*_{C-Br}	0.055	2.38	1.23 (0.9)
$CH_3CH_2CH(Br)CH_3$	2.0098		σ^*_{C-Br}	0.041	2.26	1.25 (0.9)
cyclopropylbromide	1.9437		σ^*_{C-Br}	0.119	2.44	1.20 (0.84)
cyclopentylbromide	2.0084		σ^*_{C-Br}	0.101	2.32	1.20 (1.0)
cyclohexylbromide	2.0018		σ^*_{C-Br}	0.109	2.19	1.30 (1.1)
$(CH_3)_3CBr$	2.0333		σ^*_{C-Br}	−0.072	2.13	1.09 (0.75)
$H_2C=CH_2$		1.3308	σ^*_{C-C}	3.331		
			π^*_{CC}	0.512 (1.62)	3.34	1.73[c]
$H_2C=CHBr$	1.9075	1.3265	σ^*_{C-Br}	0.333		
			π^*_{CC}	−0.073 (1.15)	2.46	1.17 (0.66)
cis $CH_3CH=CHBr$	1.9107	1.3305	σ^*_{C-Br}	0.549		
			π^*_{CC}	0.117 (1.31)	2.46	1.49 (0.55)
trans $CH_3CH=CHBr$	1.9097	1.3297	σ^*_{C-Br}	0.405		
			π^*_{CC}	0.019 (1.23)	2.67 (σ^*)	1.30 (0.60)
$H_2C=C(Br)CH_3$	1.9310	1.3298	σ^*_{C-Br}	0.180		
			π^*_{CC}	0.013 (1.22)	2.33	1.31 (0.98)
$H_2C=CHCH_2Br$	2.0040	1.3345	$\pi^*-\sigma^*$	0.982		2.34 (0.78)
			$\pi^*+\sigma^*$	−0.779 (0.58)	1.45	0.60 (0.52)
$CH_3CH=CHCH_2Br$	2.0126	1.3378	$\pi^*-\sigma^*$	1.191		2.25 (0.74)
			$\pi^*+\sigma^*$	−0.653 (0.69)	1.47	0.68 (0.56)
3-Br-cyclohex-1-ene	2.0185	1.3386	$\pi^*-\sigma^*$	0.793		2.25 (0.8)
			$\pi^*+\sigma^*$	−0.466 (0.83)	1.57	0.70 (0.54)
$H_2C=CH(CH_2)_2Br$	1.9836	1.3335	$\pi^*-\sigma^*$	0.907		1.60 (0.7)
			$\pi^*+\sigma^*$	−0.374 (0.91)	1.64	0.92 (0.60)
$H_2C=CH(CH_2)_3Br$	1.9835	1.3331	π^*_{CC}	0.478 (1.60)		1.59 (0.85)
			σ^*_{C-Br}	0.041	1.98 (σ^*)	1.2 (est.)
$H_2C=CH(CH_2)_4Br$	1.9888	1.3333	π^*_{CC}	0.625 (1.71)		1.58 (0.80)
			σ^*_{C-Br}	0.117	2.05 (σ^*)	1.2 (est.)

[a] The experimental VAEs are also reported for comparison. All energies are in eV. [b] From ref 22. [c] From ref 35.

between the carbon atoms involved in the double bond. A decrease or increase in these distances would cause a destabilization or a stabilization, respectively, of the empty MOs, owing to their antibonding character.

The calculated bond distances are given in Table 1. The C(1)−C(2) double bond length is predicted to remain nearly constant (1.334 ± 0.005 Å) in ethene and the bromoalkenes, except for vinyl bromide (1.3265 Å).

In the saturated compounds, the C−Br bond length increases slightly on going from the normal (1.99 Å) to the secondary bromides (both linear and cyclic, 2.00−2.01 Å) and *tert*-butylbromide (2.03 Å). Only in cyclopropylbromide the C−Br distance is sizeably smaller (1.9437 Å). In the unsaturated derivatives where the double bond and the bromine atom are separated by one (maximum σ^*/π^* admixture) or more CH_2 groups, the C−Br distance is close to that of the saturated bromides, ranging from 1.98 to 2.02 Å. In contrast, in vinylbromide and its methyl derivatives, where the bromine atom is bonded to a carbon atom of the double bond, the C−Br bond length (1.91−1.93 Å) is significantly shorter. Other conditions being the same, this factor causes an energy increase of the σ^*_{C-Br} MO.

Another important structural parameter in the ethene derivatives is the conformation. The crucial requirement for the occurrence of maximum π^*/σ^*_{C-Br} mixing (the π^* and σ^* labels are used in a local sense) is that the C(3)−C(4) bond (or the C(3)−Br(4) bond in 3-Br-1-enes) lies out of the C(1)−C(2)−C(3) plane, the orientation of the other σ bonds being less important. In allylbromide and its methyl derivative 4-Br-2-butene, the calculated C(1)−C(2)−C(3)−Br(4) dihedral angles are 117° and 114°, respectively, indicating the occurrence of strong interaction between the π^* and the σ^*_{C-Br} MOs, whereas a somewhat larger dihedral angle (137°) is predicted for 3-Br-cyclohexene. The C(1)−C(2)−C(3)−C(4) dihedral angle in the compounds where the double bond and the bromine atom are separated by two or more CH_2 groups is calculated to be 114° in 4-Br-1-butene and 118° in 5-Br-1-pentene and 6-Br-1-hexene.

ET Spectra. Figure 1 reports the ET spectra in the 0−6 eV range of normal, secondary (linear and cyclic) bromoalkanes, and *tert*-butylbromide. The measured VAEs and widths (full width half-maximum, i.e., energy separation between minimum and maximum of the derivatized signal) are given in Table 1. The spectra of 1-Br-ethane, -propane, and -butane display a rather broad (about 1.2 eV) resonance centered at 1.3 eV, to be compared with 2.4 eV in the chlorine analogues.[20] In the secondary 2-Br-propane and -butane and the cyclic propyl and pentyl derivatives, the energy of the σ^*_{C-Br} resonance is about 1.2 eV, despite the significantly smaller C−Br distance in cyclopropylbromide, whereas a slightly higher VAE (1.30 eV) is measured in cyclohexylbromide. In the chloro analogues, an even higher VAE increase (0.3−0.4 eV) of the cylohexyl derivative was found.[23] The VAE (1.09 eV) measured in *tert*-butylbromide is equal within experimental limits to the one (1.12 eV) previously reported.[36] The ET spectra of cyclopropyl-, cyclopentyl- and *tert*-butylbromide also display a second distinct resonance at 4.5, 5.3, and 3.9 eV, respectively.

It is to be noticed that the stabilization (0.2 eV) of the first anion state on going from the 1-Br-alkanes to *tert*-butylbromide is substantially smaller than that (0.6 eV) observed in the corresponding chlorides.[20] This is consistent with the sizeably lower energy of the σ^*_{C-Br} MO and the consequent lesser sensitivity to mixing with the higher-lying σ^*_{C-C} orbitals.

The energies of the σ^*_{C-Br} LUMOs obtained with B3LYP/6-31G* calculations for the neutral states of the 1-Br-alkanes

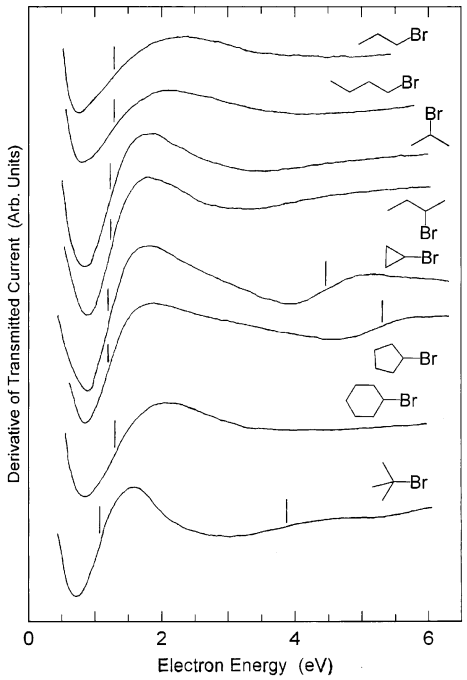

Figure 1. Derivative of transmitted current, as a function of electron energy, in 1-Br-propane, 1-Br-butane, 2-Br-propane, 2-Br-butane, cyclopropyl-, cyclopentyl-, and cyclohexylbromide, and *tert*-butylbromide. The vertical lines locate the VAEs.

and *tert*-butylbromide differ by 0.2 eV (see Table 1), in quite good agreement with the experimental VAEs, although the slightly higher VAE of cyclohexylbromide among the secondary bromides is not reproduced. Table 1 also reports the VAEs calculated as the energy difference between the lowest anion and the neutral state (both in the optimized geometry of the latter). The calculated values are about 1 eV higher than the experimental VAEs and the predicted stabilization (0.4 eV) of the first anion state on going from the normal bromides to *tert*-butylbromide is also overestimated.

Figure 2, parts A and B, reports the ET spectra of vinyl bromide and methyl derivatives (where the bromine atom is attached to the double bond and π^*/σ^*_{C-Br} mixing is forbidden for symmetry reasons in the rigid equilibrium geometry of the neutral state), allyl bromide and alkyl derivatives (where the largest π^*/σ^*_{C-Br} mixing occurs), and 4-Br-1-butene, 5-Br-1-pentene, and 6-Br-1-hexene, where the double bond and the bromine atom are separated by two or more CH_2 groups and coupling between the π^* and σ^*_{C-Br} through the intermediate σ^*_{C-C} MOs is expected to decrease rapidly.

The spectra of vinyl bromide, cis and trans 1-Br-1-propene and 2-Br-1-propene display a single distinct resonance, suggesting that the intense π^* signal masks the (close in energy) weaker and broader σ^*_{C-Br} signal. The π^* VAE (1.17 eV) measured in vinyl bromide is in quite good agreement with the value (1.16 eV) previously reported in the literature.[10] The stabilization with respect to unsubstituted ethene (AE = 1.73 eV[35]) is likely to be ascribed to the electron-withdrawing inductive effect of the halogen atom. The VAEs (1.3 eV, see Table 1) of trans 1-Br-1-propene and 2-Br-1-propene are in line with the destabilizing effect caused by methyl substitution on small π-molecular systems such as ethene or formaldehyde[3]. The significantly higher VAE (1.49 eV) of the cis isomer of 1-Br-1-propene is not easily explainable on a qualitative basis (and according to the calculated geometries is not to be ascribed to a shortening of the double bond length). The calculated π^* VOEs, however, parallel the experimental trend.

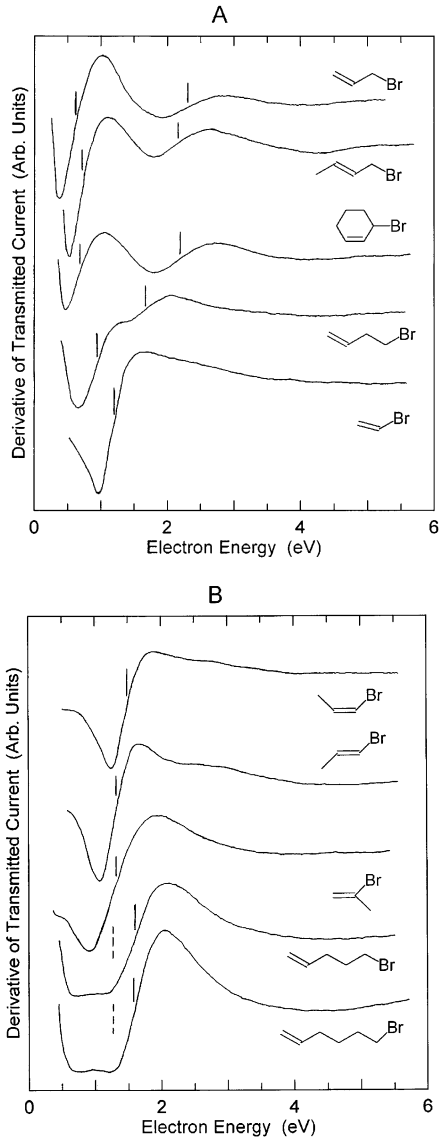

Figure 2. Derivative of transmitted current, as a function of electron energy, in A) allyl bromide (3-Br-1-propene), 4-Br-2-butene, 3-Br-cyclohexene, 4-Br-1-butene; B) cis 1-Br-1-propene, trans 1-Br-1-propene, 2-Br-propene, 5-Br-1-pentene, and 6-Br-1-hexene. The vertical lines locate the VAEs. The dashed lines refer to estimated σ^* VAEs.

The B3LYP calculations predict the C−Br distance in these compounds, where the bromine atom is attached to an ethene double bond carbon, to be 0.08 Å shorter with respect to the corresponding saturated derivatives and, in agreement, a slightly higher energy of the σ^*_{C-Br} MO. In particular, as a result of this destabilization and the inductive stabilization experienced by the π^* MO, the calculated σ^*_{C-Br} MO (see Table 1) is predicted to lie about 0.4 eV above the π^* MO, the energy difference being reduced to 0.2 eV in 2-Br-1-propene. The calculated VOEs are thus in nice agreement with the absence of a distinct σ^* resonance in the ET spectra of these compounds.

The ET spectrum of 3-Br-1-propene displays two resonances at 0.60 and 2.34 eV, and similar spectra are observed for its alkyl derivatives 4-Br-2-butene and 3-Br-cyclohexene.

Owing to the energy proximity of the interacting MOs, σ^*/π^* admixture is even stronger than in allyl chloride (VAE = 1.01 eV[19]), the first two anion states being localized at both the ethene and C−Br bonds. A picture of the LUMO, as supplied by the B3LYP calculations, is reported in Figure 3. As a consequence of its large π^* character, the second resonance is

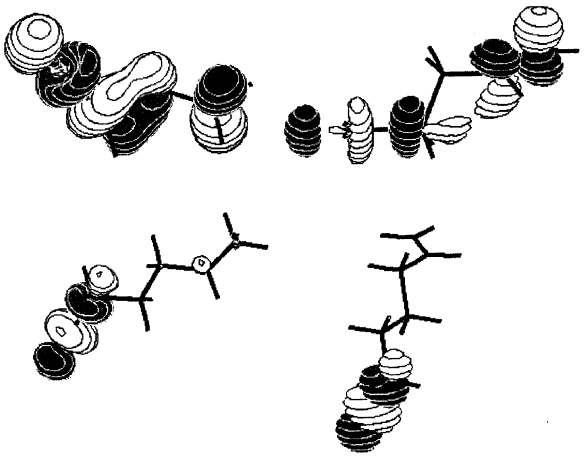

Figure 3. Representation of the LUMO, as supplied by the B3LYP/6-31G* calculations, of allyl bromide, 4-Br-1-butene, 5-Br-1-pentene, and 6-Br-1-hexene.

significantly narrower (fwhm <0.8 eV, see Table 1) than the σ^* resonance of the normal and secondary bromoalkanes, despite its higher energy.

In 4-Br-1-butene, two CH_2 groups separate the π^* and σ^*_{C-Br} MOs. As previously pointed out in the literature,[16−19] the higher-lying intermediate empty σ^*_{C-C} MOs are inefficient in promoting through-bond coupling of the π^* MO with a remote $\sigma^*_{C-halogen}$ MO. For instance, the ET spectrum of $C_6H_5-CH_2CH_2Cl$[17] displays a single low-energy resonance due to the unresolved contributions of both the components of the benzene e_{2u} (π^*) LUMO, indicating that weak interaction with the σ^* MOs removes only slightly their degeneracy.

Therefore, 4-Br-1-butene could be expected to possess localized and close in energy π^* and σ^*_{C-Br} MOs and to give rise to an ET spectrum similar to that of vinyl bromide. In contrast, the ET spectrum (see Figure 2A) displays two resolved resonances at 0.92 and 1.60 eV, their assignment to the corresponding π^* and σ^* MOs not being straightforward. This finding is accounted for by the B3LYP calculations, which predict the LUMO to be about 0.3 eV more stable than that of vinyl bromide with a sizably larger energy separation between the first two empty MOs (see Table 1). Interestingly, the calculated localization properties show that each of the first two empty MOs possesses about equal π^* and σ^*_{C-Br} character. A representation of the LUMO is given in Figure 3. According to this picture, in agreement with the above considerations, σ^*/π^* mixing does not take place through the intermediate C−C bond, but directly through space. The calculated large π^* contribution to both resonances is consistent with their relatively narrow widths. It is to be noted, however, that the apparent width of the second (less intense) resonance could be reduced by partial overlap with the lower-lying resonance. For the same reason, its apparent midpoint (1.60 eV) should be considered as an upper bound to the second VAE of 4-Br-1-butene.

Finally, the ET spectra of 5-Br-1-pentene and 6-Br-1-hexene display an (intense) π^* resonance located at about 1.6 eV. The length of the alkyl chain not only reduces π^*/σ^*_{C-Br} mixing, but also attenuates the inductive effect of the bromine atom, so that the π^* VAE is only slightly smaller than that of unsubstituted ethene. At variance with the other compounds, the ET spectra clearly display another minimum on the low-energy side of the π^* resonance (see Figure 2B), which does not disappear by changing the tuning of the electrode potentials of the apparatus. We associate this feature to the low-energy extremum of the σ^*_{C-Br} resonance. In both compounds, the minimum in derivatized signal occurs at about 0.65 eV. In the normal bromoalkanes (VAE = 1.3 eV) the corresponding minimum is located at 0.74 ± 0.02 eV. From these data, the σ^* VAE in 5-Br-1-pentene and 6-Br-1-hexene can be estimated to be 1.2 eV, as shown by the dashed lines in Figure 2B. Once again, the results of the neutral state calculations nicely account for the spectral features. The LUMO is predicted to be essentially σ^*_{C-Br} in character, at about the same energy as in the saturated secondary bromides, the second empty MO (the ethene π^* MO) lying 0.4−0.5 eV above it.

As in the compounds with the bromo substituent attached to a double bond carbon atom and the chlorine analogues 5-Cl-1-pentene and 6-Cl-1-hexene, the first two empty MOs of 5-Br-1-pentene and 6-Br-1-hexene possess essentially $\sigma^*_{C-halogen}$ or ethene π^* character, but their energy ordering is reversed. This will influence the mechanism of dissociative electron attachment and production of bromide anions.

A large number of π^* VAEs measured in different classes of π systems have recently been correlated with the corresponding neutral state B3LYP/6-31G* VOEs.[19] Least mean squares treatment gave the linear equation VAE = 0.805434 × VOE + 1.21099, with a good correlation coefficient ($r = 0.993$). The lowest π^* VOEs of the present compounds have been scaled with this equation, and the predicted VAEs are reported in parentheses in Table 1. The agreement with experiment is within 0.1 eV, except for cis 1-Br-1-propene, where the extrapolated value underestimates the measured VAE by 0.2 eV.

An attempt[19] to reproduce the experimental VAEs of chloroalkenes with B3LYP calculations as the energy difference between the lowest-lying anion and the neutral state, both with geometry optimized for the neutral molecule, has shown that the use of the 6-311+G** basis set (which includes diffuse functions) often leads to an inversion of the energy ordering of π^* and σ^* anion states or to the prediction of a lowest-lying anion state associated with diffuse solutions which do not describe the physical resonance process. The 6-31G* basis set (without diffuse functions) supplies a more reliable description of the nature of the lowest anion state, even though the VAEs are overestimated by 1−2 eV.

The VAEs calculated with the 6-31G* basis set for the present bromohydrocarbons are listed in Table 1. The trend of the calculated values roughly follows the experimental one, with a difference that increases with increasing VAE. The calculated VAEs, however, do not account for the small destabilization of the π^* anion state caused by methyl substitution. In addition, the singly occupied MO of the anion is predicted to be the σ^*_{C-Br} MO not only for 5-Br-1-pentene and 6-Br-1-hexene but also for trans 1-Br-1-propene, at variance with the cis and 2-Br-isomers and vinyl bromide. This anomalous result prompted us to evaluate the VAEs of cis and trans 1-Br-1-propene with MP2/6-31G* calculations, which predicted the singly occupied MO to be the π^* MO in both cases, with a 0.1 eV higher VAE for the cis isomer, in line with the neutral state VOEs and experiment.

DEA Spectra. Most of the DEA studies reported in the literature are only concerned with the energy of the maxima observed in the cross section and the nature of the negative fragments produced, but not with the quantitative aspects, i.e., determination of the (absolute or relative) dissociative cross sections. However, such measurements supply in general very important information and become necessary for the evaluation of the efficiency of intramolecular electron-transfer processes. Our apparatus can measure the current of anions extracted from the collision chamber and mass-selected with a quadrupole filter

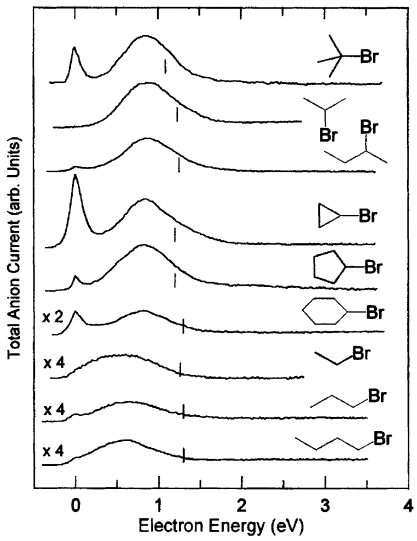

Figure 4. Total anion current, as a function of the incident electron energy, in bromoalkanes. The vertical lines locate the first VAEs measured in ETS.

TABLE 2: Peak Energies (eV) and Relative Anion Currents Measured in the DEA Spectra of Bromoalkanes and Bromoalkenes[a]

	ETS	DEAS (total anion current)		
	first VAE	peak energy	int. relative to C_6H_5Cl	int. %
CH_3CH_2Br	1.26[b]	0.6	0.15	0.8
$CH_3(CH_2)_2Br$	1.3	0.65	0.13	0.7
$CH_3(CH_2)_3Br$	1.3	0.63	0.16	0.8
$CH_3CH(Br)CH_3$	1.23	0.9	1.12	5.8
$CH_3CH_2CH(Br)CH_3$	1.25	0.85	0.83	4.3
cyclopropyl Br	1.20	0.86	1.17	6.1
cyclopentyl Br	1.20	0.85	1.17	6.1
cyclohexyl Br	1.30	0.83	0.30	1.6
$(CH_3)_3CBr$	1.09	0.86	1.20	6.2
$H_2C{=}CHBr$	1.17	1.16	3.12	16.2
cis $CH_3CH{=}CHBr$	1.49	1.51	2.58	13.4
trans $CH_3CH{=}CHBr$	1.30	1.31	0.90	4.7
$H_2C{=}C(Br)CH_3$	1.31	1.1	0.22	1.1
$H_2C{=}CHCH_2Br$	0.60	0.39	19.28	100
$CH_3C{=}CHCH_2Br$	0.68	0.40	14.64	76.0
3-Br-cyclohex-1-ene	0.70	0.41	13.49	70.0
$H_2C{=}CH(CH_2)_2Br$	0.92	0.70	0.99	5.1
$H_2C{=}CH(CH_2)_3Br$	1.2 (est.)	0.5	0.37	1.9
$H_2C{=}CH(CH_2)_4Br$	1.2 (est.)	0.5	0.30	1.6

[a] The first VAEs (eV) measured in the ET spectra are also reported for comparison. [b] From ref 22.

or, alternatively, the total anion current at the walls of the collision chamber. Although the latter can, in principle, be affected by spurious trapped electrons, these measurements are more reliable with respect to the current detected through the mass filter because of kinetic energy discrimination in the anion extraction efficiency.

Figure 4 displays the total yield of negative ions measured at the collision chamber in the saturated bromohydrocarbons, as a function of the incident electron energy, in the 0−4 eV energy range. Mass analysis revealed that (in both the bromoalkanes and -alkenes) the total anion current is essentially due only to the Br^- fragment. The measured peak energies and their intensities relative to chlorobenzene (evaluated from the peak heights normalized to the same electron beam current and pressure reading for all the compounds) are given in Table 2, where the last column also displays the percentage intensities referred to allyl bromide.

The energy threshold for Br^- formation is the difference between the C−Br dissociation energy and the EA of the bromine atom (3.14 eV in 1-Br-propane and 3.365 eV[37], respectively). Thus, the zero-energy signals in the DEA spectra may be associated with thermally excited vibrational levels of the neutral molecules and the inverse energy dependence of the electron attachment cross section for the s wave which causes the yield to climb at zero energy,[38] although contribution from traces of impurities cannot be excluded.

The complex dependence of the DEA cross section on molecular properties has been described for diatomics,[39−41] and the same concepts can be extended to polyatomics. The DEA cross section can be most simply expressed as $\sigma_{DEA} = \sigma_{CAP} \exp(-\tau_D/\tau_L)$, where σ_{CAP} is the electron capture cross section, τ_D is the time required for the nuclei to reach the separation at which the neutral and anion potential curves cross (i.e., the time required for dissociation to occur), and τ_L is the lifetime of the resonance anion state with respect to re-emission of the extra electron. In turn, τ_L depends on the symmetry and shape of the temporarily occupied MO and (in an inverse fashion) on the anion energy. The exponential factor, also referred to as the survival factor, gives the probability that the anion will live long enough to dissociate.

On this basis, the shift to lower energy of the peaks in the DEA spectra with respect to the corresponding resonances observed in ETS is well understood in terms of shorter lifetime and greater distance to the crossing between the anion and neutral potential curves for the anions formed at the high-energy side of the resonance.[39] It is to be noticed that this shift can be quite large (for instance, about 1 eV in the 1-Cl-alkanes[20]), so that the a priori assumption, sometimes met with in the literature, that the energies of the peaks observed in the DEA cross section coincide with the corresponding resonance energies is to be avoided.

In particular, in the present series, it is interesting to observe that, due to a different magnitude of the energy shift of the DEA peak from the center of the resonance, the energy of the DEA peak increases on going from the normal (0.6 eV) to the branched (about 0.85 eV) bromoalkanes, whereas the corresponding VAEs measured in the ET spectra follow the opposite trend (see Table 2 and Figure 4). This finding indicates a sizeably shorter anion lifetime (and/or a longer time required for dissociation to occur) in the normal bromoalkanes, so that only for the anions formed in the low-energy portion of the Franck−Condon envelope can dissociation compete with simple re-emission of the extra electron.

The present calibrations of the peak energies in the 1-Br-alkanes are about 0.1 eV lower than those previously obtained using the swarm-beam method.[21] In the same study, Christophorou et al.[21] also report the absolute DEA cross sections, which are approximately 30 times larger than those measured by Pearl and Burrow[23] in the corresponding normal chloroalkanes using a different experimental method. In perfect agreement with these data, we find the anion current in 1-Br-butane to be $\geq$27 times larger than that of 1-Cl-butane.[17] In the secondary and tertiary butyl derivatives, this ratio decreases to about 15−20, because the increase in the peak cross section on going from the normal to the branched alkanes is smaller in the bromides (about 7 times) than in the chlorides (about 10 times[23]), in line with the smaller VAE change in the bromides.

Comparison with the trends displayed by the DEA cross sections in the chloroalkanes[23] reveals several similarities. The anion current in 1-Br-propane is slightly smaller than in the ethyl and butyl derivatives, whereas in 2-Br-propane, it is 1.4

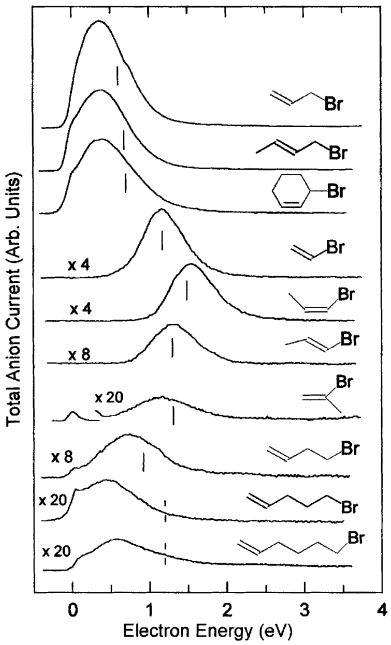

Figure 5. Total anion current, as a function of the incident electron energy, in bromoalkenes. The vertical lines locate the first VAEs measured in ETS.

times higher than in 2-Br-butane. The peak cross section of cyclohexylbromide is almost four times smaller than that of the other (linear and cyclic) secondary bromoalkenes. This decrease is likely due to the higher energy (0.1 eV) of the σ^*_{C-Br} resonance in cyclohexylbromide and its consequently shorter lifetime. Consistently, in cyclohexyl chloride where the VAE increase is larger (0.3 eV), the cross section decrease (7 times) is even more pronounced.[23] Figure 5 displays the DEA spectra of the *n*-Br-1-alkenes, with $n = 2-6$, and alkyl derivatives. The peak energies and relative cross sections are given in Table 2. The percentage Br^- yields in the *n*-Br-1-alkenes referred to allyl bromide ($n = 3$) are in very good agreement ($\pm 1\%$) with the ratios of the absolute cross sections measured by Moore and co-workers,[16] except for vinyl bromide where our relative cross section is almost twice as large. In contrast, a significant discrepancy between the two sets of data regards the magnitude of the anion current in allyl bromide relative to allyl chloride. The anion current measured here in allyl bromide is 3.0 times larger than that found[19] in allyl chloride, whereas according to previous measurements[16] this ratio is 7.9.

As expected, the largest Br^- yields are observed (see Table 2) in allyl bromide and its alkyl derivatives 4-Br-2-butene and 3-Br-cyclohexene, where strong π^*/σ^*_{C-Br} admixture takes place. Because of its low energy and π^* character, the first anion state has a relatively long lifetime which favors dissociation. Due to the large localization of the LUMO at the C−Br bond, the mechanism of Br^- production cannot be thought of as electron capture into the ethene π^* MO followed by intramolecular transfer to the bromine atom.

Alkyl substitution at the double bond of allyl bromide to give 4-Br-2-butene and 3-Br-cyclohexene reduces the peak cross section to 76% and 70%, respectively. This decrease is likely associated with the small VAE increase caused by alkyl substitution. In principle, also the larger mass could play some role by reducing the nuclear velocity along the C−Br stretching vibrational mode.

The effect of methyl substitution is confirmed on going from vinyl bromide to cis 1-Br-1-propene (see Table 2). However, the notable cross section decrease in trans 1-Br-1-propene and, mainly, 2-Br-1-propene despite their smaller VAE has no apparent explanation. In addition, in the trans isomer, as well as in the cis isomer and vinyl bromide, the energy of the DEA peak is not shifted to lower energy with respect to the center of the π^* resonance displayed in the ET spectrum, indicating that the resonance lifetime is sufficiently long for dissociation to occur. In 2-Br-1-propene, the DEA cross section is smaller than in the saturated secondary bromides, and the peak energy indicates that the process is associated with the π^* resonance.

It would be interesting to compare the C−Br out-of-plane bending vibrational frequencies (to our knowledge, not available in the literature) of these compounds where the halogen atom is bonded to an ethene carbon atom and π^*/σ^*_{C-Br} mixing (forbidden for symmetry reasons in the rigid equilibrium geometry of the neutral state) relies on vibronic coupling. A possible explanation for the large changes in the DEA cross sections, in principle, could stem from different extents of vibronic coupling.

To gain more insight to better interpret these results, we measured the peak cross section in 2-Cl-1-propene, which turned out to be five times smaller than that previously found[19] in an admixture of cis and trans isomers of 1-Cl-1-propene, in qualitative agreement with the present data on the bromides.

In 4-Br-1-butene, where the ethene group and the bromine atom are separated by two CH_2 groups, the Br^- current is about 5% relative to allyl bromide and the energy of the peak (0.70 eV) is 0.2 eV lower than the corresponding VAE (see Table 2). In 5-Br-1-pentene and 6-Br-1-hexene, the DEA cross section is <2% relative to allyl bromide and peaks at about 0.5 eV, i.e., at about the same energy as in the saturated normal bromides.

In the above-mentioned previous DEA study,[16] the decrease with chain length of the energy at the peak was interpreted in terms of a stabilization of the π^* LUMO which increases as the chain becomes longer and more flexible, noting that the peak energy in 6-Br-1-hexene is about as low as in allyl bromide.

The present ETS and B3LYP studies unveil a quite different picture. First, in 5-Br-1-pentene and 6-Br-1-hexene, the LUMO is essentially the σ^*_{C-Br} MO, the π^* MO (VAE=1.6 eV) lying at about the same energy as in unsubstituted ethene. Second, the energy of the LUMO does in fact increase from 3-Br-1-propene to 6-Br-1-hexene (then remaining presumably nearly constant for longer alkyl chains). However, although in 4-Br-1-butene the energy shift of the DEA peak relative to the corresponding resonance (VAE = 0.92 eV) is small (due to its relatively low energy and π^* component), in 5-Br-1-pentene and 6-Br-1-hexene, the Br^- current mainly derives from direct dissociation of the σ^*_{C-Br} resonance (VAE = 1.3 eV in the saturated normal bromides) and peaks at sizeably lower energy, as observed in the normal bromoalkanes.

It can be noticed that on going from 3-Cl-1-propene to 5-Cl-1-pentene the DEA cross section decreases by a factor of roughly 200,[16,19] whereas inspection of Table 2 shows that in the corresponding bromides this factor is only about 50. Moreover, in 5-Cl-1-pentene, the cross section is still 5 times larger than that of normal chlorobutane,[19] whereas in 5-Br-1-pentene, it is only twice as large as that of the normal bromoalkanes. These differences reflect the different empty level structure of the two 5-halo-1-pentenes. The energy of the ethene π^* MO is about the same (VAE = 1.6 eV) in both halopentenes, but although in 5-Cl-1-pentene the σ^*_{C-Cl} MO lies at higher energy, in 5-Br-1-pentene, the σ^*/π^* energy sequence is reversed. As a consequence, in 5-Cl-1-pentene, Cl^- production mainly derives

from electron capture into the π^* LUMO followed by intramolecular electron transfer to the chlorine atom, whereas in 5-Br-1-pentene, direct electron capture into the low-energy σ^* LUMO plays a major role compared to the π^*-to-σ^* electron-transfer mechanism.

In the unsaturated chlorides $X-(CH_2)_3Cl$, the relative Cl^- yields were found[19] to be 5:2:1 for $X = C_6H_5$, $H_2C{=}CH$, and $HC{\equiv}C$, respectively. The above findings lead to the prediction that in the corresponding bromides the Br^- current should be less affected by the nature of the π system.

Conclusions

In the present work, we have shown the connection between dissociative electron attachment cross section (peak energy and magnitude) and the empty level structure of bromoalkanes and bromoalkenes.

The neutral state virtual orbital energies supplied by B3LYP/6-31G* calculations account for the resonances observed in the ET spectra and satisfactorily reproduce the experimental attachment energy trends.

In the saturated bromohydrocarbons, the energy of electron attachment to the lowest-lying empty σ^* MO (1.3 eV in normal bromides, 1.1 eV in tertbutyl bromide) is about 1 eV lower than that of the corresponding chlorides and less sensitive to branching. With respect to the chloro analogues, the DEA cross sections of the normal and branched bromoalkanes are about 30 times and 15−20 times larger, respectively.

In the ET spectra of vinylbromide and its methyl derivatives, the π^* and (weaker) σ^*_{C-Br} resonances are not resolved. According to the calculations, the ethene π^* MO lies at about 0.3 eV lower energy than the σ^*_{C-Br} MO. In agreement, the Br^- current in the DEA spectra peaks at an energy close to that of the π^* resonance observed in the ET spectra. In these compounds, where π^*/σ^*_{C-Br} mixing (forbidden for symmetry reasons in the equilibrium geometry of the neutral molecule) relies on vibronic coupling, the magnitude of the DEA cross section seems to be strongly influenced by substitution at the double bond.

In 5-Br-1-pentene and 6-Br-1-hexene, where the intermediate CH_2 groups prevent large π^*/σ^*_{C-Br} admixture, the calculations predict the reversed energy ordering, i.e., the LUMO is predicted to be the σ^*_{C-Br} MO. This result is supported by experiment. The ET spectra do not display two resolved resonances, but a shoulder can be observed at the low-energy side of the (more intense) π^* resonance. Moreover, the DEA cross section peaks at 0.5 eV (compared to 1.2 eV in vinyl bromide), namely, at about the same energy as in the normal bromoalkanes, where the maximum of the Br^- current is sizeably shifted to lower energy with respect to the center of the σ^* resonance observed in ETS.

The latter results point out a substantial difference with respect to the empty level structure of the corresponding chloroalkenes, where the σ^*_{C-Cl} MO lies at higher energy than the ethene π^* MO. As a consequence, in chloropentene and hexene, the mechanism of Cl^- production mainly proceeds through electron capture into the π^* LUMO, followed by intramolecular electron transfer to the C−Cl bond, whereas in the bromides $H_2C{=}CH-(CH_2)_nBr$ with $n > 2$, the major role is played by direct dissociation of the (lower-lying) σ^* resonance.

Acknowledgment. Thanks are due to the Italian Ministero dell'Istruzione, dell'Università e della Ricerca and the University of Bologna (Funds for Selected Topics) for financial support.

References and Notes

(1) Massey, H. S. W., McDaniel, E. W., Bederson, B., Eds.; *Applied Atomic Collision Physic;* Academic Press: New York, 1984; Vols. 1−5.
(2) Sanche, L.; Schulz, G. J. *Phys. Rev. A* **1972**, *5*, 1672.
(3) Jordan, K. D.; Burrow, P. D. *Acc. Chem. Res.* **1978**, *11*, 341.
(4) Schulz, G. J. *Rev. Mod. Phys.* **1973**, *45*, 378, 423.
(5) Illenberger, E.; Momigny, J. *Gaseous Molecular Ions. An Introduction to Elementary Processes Induced by Ionization*; Steinkopff Verlag Darmstadt, Springer-Verlag: New York, 1992.
(6) Ward, M. D. *Chem. Soc. Rev.*, **1995**, *24*, 121.
(7) Dressler, R.; Allan, M.; Haselbach, E. *Chimia* **1985**, *39*, 385.
(8) Stricklett, K. L.; Chiu, S. C.; Burrow, P. D. *Chem. Phys. Lett.* **1986**, *131*, 279.
(9) Modelli, A.; Foffani, A.; Scagnolari, F.; Jones, D. *Chem. Phys. Lett.* **1989**, *163*, 269.
(10) Olthoff, J. K.; Tossell, J. A.; Moore, J. H. *J. Chem. Phys.* **1985**, *83*, 5627.
(11) Christophorou, L. G.; Compton, R. N.; Hurst, G. S.; Reinhardt, P. W. *J. Chem. Phys.* **1966**, *45*, 536.
(12) Kaufel, R.; Illenberger, E.; Baumgärtel, H. *Chem. Phys. Lett.* **1984**, *106*, 342.
(13) Bulliard, C.; Allan, M.; Haselbach, E. *J. Phys. Chem.* **1994**, *98*, 11040.
(14) Pearl, D. M.; Burrow, P. D.; Nash, J. J.; Morrison, H.; Jordan, K. D. *J. Am. Chem. Soc.* **1993**, *115*, 9876.
(15) Pearl, D. M.; Burrow, P. D.; Nash, J. J.; Morrison, H.; Nachtigallova, D.; Jordan, K. D. *J. Phys. Chem.* **1995**, *99*, 12379.
(16) Underwood-Lemons, T.; Saghi-Szabo, G.; Tossell, J. A.; Moore, J. H. *J. Chem. Phys.* **1996**, *105*, 7896.
(17) Modelli, A.; Venuti, M. *J. Phys. Chem. A* **2001**, *105*, 5836.
(18) Modelli, A.; Venuti, M.; Szepes, L. *J. Am. Chem. Soc.* **2002**, *124*, 8498.
(19) Modelli, A. *Phys. Chem. Chem. Phys*. **2003**, *5*, 2923.
(20) Guerra, M.; Jones, D.; Distefano, G.; Scagnolari, F.; Modelli, A. *J. Chem. Phys.* **1991**, *94*, 484.
(21) Christophorou, L. G.; Carter, J. G.; Collins, P. M.; Christodoulides, A. A. *J. Chem. Phys*. **1971**, *54*, 4706.
(22) Modelli, A.; Scagnolari, F.; Distefano, G.; Jones, D.; Guerra, M. *J. Chem. Phys*. **1992**, *96*, 2061.
(23) Pearl, D. M.; Burrow, P. D. *J. Chem. Phys.* **1994**, *101*, 2940. Aflatooni, K.; Burrow, P. D. *J. Chem. Phys*. **2000**, *96*, 1455.
(24) Staley, S. W.; Strnad, J. T. *J. Phys. Chem.* **1994**, *98*, 161.
(25) Chao, J. S−Y.; Falcetta, M. F.; Jordan, K. D. *J. Chem. Phys.* **1990**, *93*, 1125.
(26) Burrow, P. D.; Howard, A. E.; Johnston, A. R.; Jordan, K. D. *J. Phys. Chem.* **1992**, *96*, 7570.
(27) Venuti, M.; Modelli, A. *J. Chem. Phys.* **2000**, *113*, 2159.
(28) Koopmans, T. *Physica (Amsterdam)* **1934**, *1*, 104.
(29) Modelli, A.; Martin, H. D. *J. Phys. Chem. A* **2002**, *106*, 7271.
(30) Modelli, A.; Distefano, G.; Jones, D. *Chem. Phys.* **1982**, *73*, 395.
(31) Johnston, A. R.; Burrow, P. D. *J. Electron Spectrosc. Relat. Phenom.* **1982**, *25*, 119.
(32) Modelli, A.; Guerra, M.; Jones, D.; Distefano, G.; Tronc, M. *J. Chem. Phys*. **1998**, *108*, 9004.
(33) Frisch, M. J.; Trucks, G. W.; Schlegel, H. B.; Scuseria, G. E.; Robb, M. A.; Cheeseman, J. R.; Zakrzewski, V. G.; Montgomery, J. A., Jr.; Stratmann, R. E.; Burant, J. C.; Dapprich, S.; Millam, J. M.; Daniels, A. D.; Kudin, K. N.; Strain, M. C.; Farkas, O.; Tomasi, J.; Barone, V.; Cossi, M.; Cammi, R.; Mennucci, B.; Pomelli, C.; Adamo, C.; Clifford, S.; Ochterski, J.; Petersson, G. A.; Ayala, P. Y.; Cui, Q.; Morokuma, K.; Malick, D. K.; Rabuck, A. D.; Raghavachari, K.; Foresman, J. B.; Cioslowski, J.; Ortiz, J. V.; Stefanov, B. B.; Liu, G.; Liashenko, A.; Piskorz, P.; Komaromi, I.; Gomperts, R.; Martin, R. L.; Fox, D. J.; Keith, T.; Al-Laham, M. A.; Peng, C. Y.; Nanayakkara, A.; Gonzalez, C.; Challacombe, M.; Gill, P. M. W.; Johnson, B. G.; Chen, W.; Wong, M. W.; Andres, J. L.; Head-Gordon, M.; Replogle, E. S.; Pople, J. A. *Gaussian 98*, revision A.6; Gaussian, Inc.: Pittsburgh, PA, 1998.
(34) Becke, A. D. *J. Chem. Phys.* **1993**, *98*, 5648.
(35) Burrow, P. D.; Modelli, A.; Chiu, N. S. *Chem. Phys. Lett.* **1981**, *82*, 270.
(36) Modelli, A.; Scagnolari, F.; Distefano, G.; Guerra, M.; Jones, D. *Chem. Phys.* **1990**, *145*, 89.
(37) Chen, E. C. M.; Albyn, K.; Dussack, L.; Wentworth, W. E. *J. Phys. Chem.* **1989**, *93*, 6827.
(38) Chutjian, A.; Alajajian, S. H. *Phys. Rev. A* **1985**, *31*, 2885.
(39) O'Malley, T. F. *Phys. Rev.* **1966**, *150*, 14.
(40) Bardsley, J. N.; Herzenberg, A.; Mandl, F. *Proc. Phys. Soc. London* **1966**, *89*, 321.
(41) Chen, J. C. Y. *Phys. Rev.* **1966**, *148*, 66.